UNCLASSIFIED

TM No.
TC- 173-72

NAVAL UNDERWATER SYSTEMS CENTER

Technical Memorandum

SIGNAL PROCESSING IN REVERBERATION- A SUMMARY OF PERFORMANCE CAPABILITY

Date: 30 August 1972

Prepared by: Albert H. Nuttall
Albert H. Nuttall
Office of the Director of
Science and Technology

Approved for public release; distribution unlimited

UNCLASSIFIED

UNCLASSIFIED

TM No.
TC-173-72

NAVAL UNDERWATER SYSTEMS CENTER

Technical Memorandum

SIGNAL PROCESSING IN REVERBERATION- A SUMMARY OF PERFORMANCE CAPABILITY

Date: 30 August 1972

Prepared by: Albert H. Nuttall

Albert H. Nuttall
Office of the Director of
Science and Technology

Approved for public release; distribution unlimited

UNCLASSIFIED

TM No.
TC-173-72

NAVAL UNDERWATER SYSTEMS CENTER
Newport, Rhode Island 02840

ABSTRACT

Some of the fundamental limitations and features of signal processing in a simple reverberation environment are given, along with the important derivations and assumptions. Emphasis on periodically-pulsed trains is made, and various suboptimum processors are considered, along with their performance capability.

ADMINISTRATIVE INFORMATION

This memorandum was prepared under Project No. A75205, Sub-Project No. ZF61 112001, "Statistical Communication with Applications to Sonar Signal Processing," Principal Investigator Dr. A. H. Nuttall, Code TC. The sponsoring activity is Chief of Naval Material, Program Manager Dr. J. H. Huth.

The author of this memorandum is located at the New London Laboratory, Naval Underwater Systems Center, New London, Connecticut 06320.

TABLE OF CONTENTS

1. INTRODUCTION

These notes are the result of an (incomplete) literature search of recent work on optimum signal processing in reverberation. Relevant material to acoustic signal processing has been extracted and compiled in a consistent set of notations. Some important technical aspects of sub-optimum processing for pulsed trains in a simple reverberation environment are brought out.

2. SIGNAL, REVERBERATION, AND NOISE MODELS

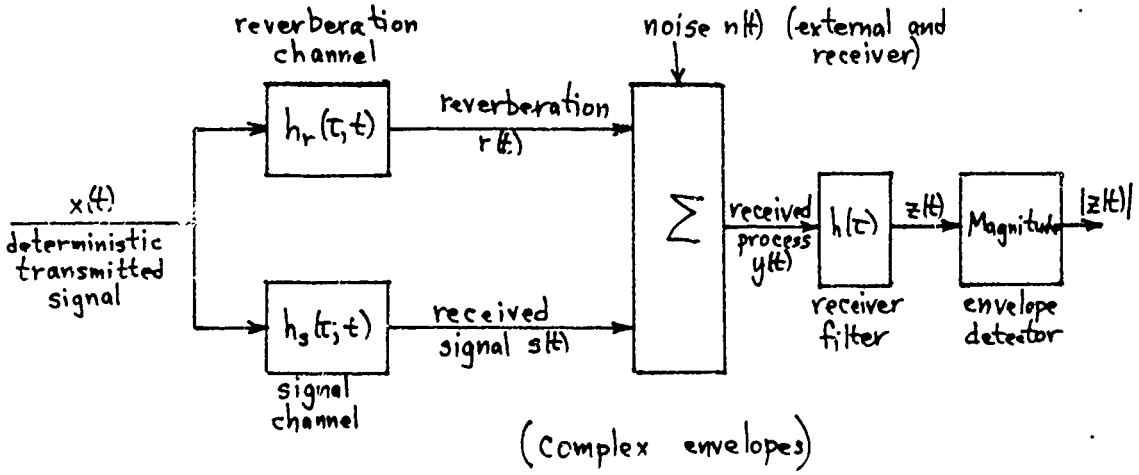

Figure 1. Medium and Receiver Block Diagram

A generic block diagram of the system under investigation here is given in Figure 1. The deterministic transmitted signal is presumed to be narrowband and is characterized by its complex envelope $x(t)$ (see Ref. 1, App. A, for example, for the notation to be used). Although only one narrowband receiver filter, $h(\tau)$, is depicted in Figure 1, it is but one out of a bank of filters that would be used in practice, in order to cover the expected Doppler shifts. The time-varying impulse responses

$$h_s(\tau;t) \quad \text{and} \quad h_r(\tau;t) \tag{1}$$

of the signal and reverberation channels in Figure 1 are the responses at time t to a unit impulse applied τ ago (Ref. 2).

2.1 Received Signal Characteristics

For multipath and doppler in the signal channel of Figure 1, we have, if a target is present,

$$h_s(\tau, t) = \sum_k V_k \, \delta(\tau - t_{d_k}) \exp(i2\pi f_{d_k} t), \tag{2}$$

where t_{d_k} and f_{d_k} are the time delay and frequency shift of the k-th path, and V_k is the complex voltage gain* (attenuation and phase shift) of the k-th path in the signal channel. (If there is no target, the $\{V_k\}$ are zero. This model is capable of including multiple targets as well.) The signal channel includes the effects of the medium and the target. (The spreading function (Ref. 2) of the signal channel is

$$a_s(\tau, \nu) = \sum_k V_k \, \delta(\tau - t_{d_k}) \, \delta(\nu - f_{d_k}) \tag{3}$$

Then the received signal

$$\begin{aligned} s(t) &= \tfrac{1}{2} \int d\tau \, h_s(\tau, t) \, x(t - \tau) \\ &= \tfrac{1}{2} \sum_k V_k \, x(t - t_{d_k}) \exp(i2\pi f_{d_k} t). \end{aligned} \tag{4}$$

The signal component of receiver filter output $z(t)$ in Figure 1 is

$$\begin{aligned} z_s(t) &= \tfrac{1}{2} \int d\tau \, h(\tau) \, s(t - \tau) \\ &= \tfrac{1}{2} \int d\tau \, h(\tau) \, \tfrac{1}{2} \sum_k V_k \, x(t - \tau - t_{d_k}) \exp[i2\pi f_{d_k}(t - \tau)]. \end{aligned} \tag{5}$$

Define the cross-ambiguity function of transmitted signal and receiver filter as

$$\chi_{xh}(\tau, \nu) = \int dt \, x(t + \tau) h(-t) e^{-i2\pi\nu t} = \int df \, e^{i2\pi f \tau} X(f) H(f - \nu). \tag{6}$$

---

*$|V_k| = 2R_k$, where R_k is the real voltage gain applied to the high-frequency narrowband signals in the k-th path of the signal channel.

Then

$$z_s(t) = \frac{1}{4}\sum_k V_k \, e^{i2\pi f_{d_k} t} \, \chi_{xh}(t - t_{d_k}, -f_{d_k}). \tag{7}$$

Thus cross-ambiguity function χ_{xh} is displaced in time and frequency and added (with complex factors) to obtain the signal output waveform of the receiver filter.

(For a single path,

$$s(t) = \tfrac{1}{2} V \, x(t - t_d) \, e^{i2\pi f_d t},$$

$$S(f) = \tfrac{1}{2} V \, X(f - f_d) \exp\left[-i2\pi (f - f_d) t_d\right],$$

$$z_s(t) = \tfrac{1}{4} V \chi_{xh}(t - t_d, -f_d) \, e^{i2\pi f_d t}.) \tag{8}$$

The transmitted signal energy is

$$E_x = \tfrac{1}{2}\int dt \, |x(t)|^2.$$

The received signal energy in the k-th path is, from (4),

$$E_{s_k} = \tfrac{1}{2}\int dt \left| \tfrac{1}{2} V_k \, x(t - t_{d_k}) \exp(i2\pi f_{d_k} t) \right|^2$$

$$= \tfrac{1}{8}|V_k|^2 \int dt \, |x(t - t_{d_k})|^2 = \tfrac{1}{4}|V_k|^2 E_x = R_k^2 E_x. \tag{9}$$

R_k^2 is the real power gain of the k-th path in the signal channel; it represents the fraction of transmitted signal energy that is received.

2.2 Reverberation Characteristics

The reverberation waveform at the receiver input is given by

$$r(t) = \tfrac{1}{2}\int d\tau \, h_r(\tau, t) \, x(t - \tau). \tag{10}$$

We assume that $h_r(\tau, t)$ is a member function of an ensemble with statistical property

$$\overline{a_r(\tau_1, \nu_1) \, a_r^*(\tau_2, \nu_2)} = \sigma_r(\nu_1, \tau_1) \, \delta(\tau_1 - \tau_2) \, \delta(\nu_1 - \nu_2). \tag{11}$$

This is the uncorrelated scatterer channel; σ_r is the scattering function of the reverberation channel (see Ref. 2). Then

$$\overline{h_r(\tau_1, t_1) h_r^*(\tau_2, t_2)} = \delta(\tau_1 - \tau_2) \int d\nu \, e^{i2\pi\nu(t_1 - t_2)} \sigma_r(\nu, \tau_1). \tag{12}$$

The reverberation process r(t) is not stationary; its correlation at time t is defined as

$$R_r(\tau, t) = \overline{r(t + \tfrac{\tau}{2}) r^*(t - \tfrac{\tau}{2})}$$

$$= \tfrac{1}{4} \iint d\tau_1 d\tau_2 \, \overline{h_r(\tau_1, t + \tfrac{\tau}{2}) h_r^*(\tau_2, t - \tfrac{\tau}{2})} \, x(t + \tfrac{\tau}{2} - \tau_1) x^*(t - \tfrac{\tau}{2} - \tau_2)$$

$$= \tfrac{1}{4} \iint d\tau_1 \, d\nu \, e^{i2\pi\nu\tau} \sigma_r(\nu, \tau_1) x(t + \tfrac{\tau}{2} - \tau_1) x^*(t - \tfrac{\tau}{2} - \tau_1). \tag{13}$$

We now assume that the reverberation scattering σ_r changes slowly with range (delay τ). Then considering the integral on τ_1 in more detail, if $\sigma_r(\nu, \tau_1)$

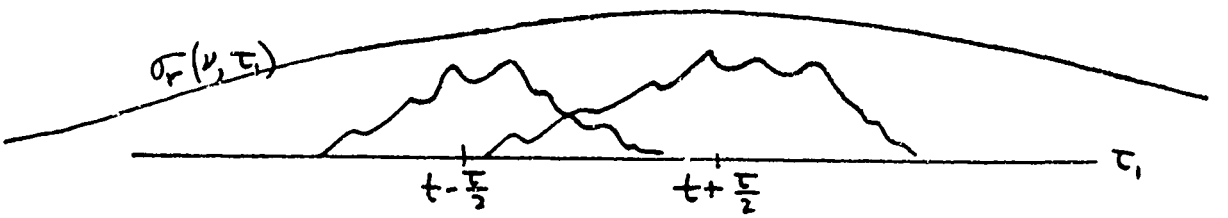

Figure 2. τ_1 - integration in Equation (13)

changes but slightly versus τ_1 in the signal duration, then the integral on τ_1 in (13) is approximately

$$\sigma_r(\nu, t) \int d\tau_1 \, x(t + \tfrac{\tau}{2} - \tau_1) x^*(t - \tfrac{\tau}{2} - \tau_1)$$

$$= \sigma_r(\nu, t) \int du \, x(u) x^*(u - \tau). \tag{14}$$

Then (13) gives

$$R_r(\tau, t) = \tfrac{1}{4} \int du \, x(u) x^*(u - \tau) \int d\nu \, e^{i2\pi\nu\tau} \sigma_r(\nu, t). \tag{15}$$

Now reverberation correlation $R_r(\tau, t)$ varies slowly with time t, as seen from (15); therefore a time-varying reverberation spectrum can be defined as

$$G_r(f,t) = \int d\tau \; e^{-i2\pi f\tau} R_r(\tau,t)$$

$$= \frac{1}{4} |X(f)|^2 \circledast \sigma_r(f,t), \tag{16}$$

using (15).

That is, the reverberation spectrum is the convolution of the transmitted signal energy density spectrum with the scattering function of the reverberation channel.

The real power in the reverberation is

$$P_r(t) = \frac{1}{2}\overline{|r(t)|^2} = \frac{1}{2}\int df\, G_r(f,t) = \frac{1}{2}\int df\, \frac{1}{4}\int du\, |X(f-u)|^2 \sigma_r(u,t)$$

$$= \frac{1}{4} E_x \int du\, \sigma_r(u,t). \tag{17}$$

The reverberation power depends on the transmitted signal only through its energy, and not on its time structure or duration, or its frequency structure or bandwidth. Thus if the transmitted signal bandwidth is widened, the average reverberation spectrum level will decrease, for a fixed transmitted signal energy. On the other hand, for a power-limited transmitter, the reverberation power is seen to be directly proportional to the signal duration.

2.3 Noise Characteristics

The received noise, whether external or receiver noise, is assumed to be stationary with spectrum $G_n(f)$.

3. RECEIVER PROCESSOR

We allow an infinite observation time at the receiver. Also suppose there is just one path in the signal channel. We define the instantaneous signal output in $z(t)$ at sample instant t_0 as the envelope sample $|z_s(t_0)|$. The squared-envelope, which is a measure of output signal power, is

$$|z_s(t_0)|^2 = \frac{1}{16}|V|^2 \left|\chi_{xh}(t_0 - t_d, -f_d)\right|^2$$

$$= \frac{R^2}{4}\left|\int df \exp[i2\pi f(t_0 - t_d)]\, X(f)\, H(f+f_d)\right|^2$$

$$= \frac{R^2}{4}\left|\int df \exp[i2\pi f(t_0 - t_d)]\, X(f-f_d)\, H(f)\right|^2, \tag{18}$$

from (8), (6), and (9).

The total interference power output at sample instant t_0 from the receiver filter is

$$\frac{1}{2}\overline{|z_r(t_0) + z_n(t_0)|^2}$$

$$= \frac{1}{2}\left[\overline{|z_r(t_0)|^2} + \overline{|z_n(t_0)|^2}\right]$$

$$= \frac{1}{8}\int df \left[G_r(f, t_0) + G_n(f)\right] |H(f)|^2. \tag{19}$$

The output signal-to-total-interference ratio (SIR) at time t_0 is given by the ratio of (18) to (19):

$$SIR = 2R^2 \frac{\left|\int df \exp[i2\pi f(t_0 - t_d)]\, X(f-f_d)\, H(f)\right|^2}{\int df \left[G_r(f, t_0) + G_n(f)\right] |H(f)|^2}. \tag{20}$$

(If only a limited frequency band W is allowed, the integrals in (20) and the following only extend over that band W).

This quantity is maximized by the choice of receiving filter $H(f)$ as

$$H_0(f) = \frac{X^*(f-f_d)\exp[-i2\pi f(t_0 - t_d)]}{G_r(f, t_0) + G_n(f)}. \tag{21}$$

This is also the optimum processor when reverberation and noise are Gaussian processes. $G_r(f,t)$ is given by (16). This filter is seen to depend on sampling time instant t_0 and frequency shift f_d. However, the exponential is merely a delay term. Also, the remainder could be approximately realized physically as follows:

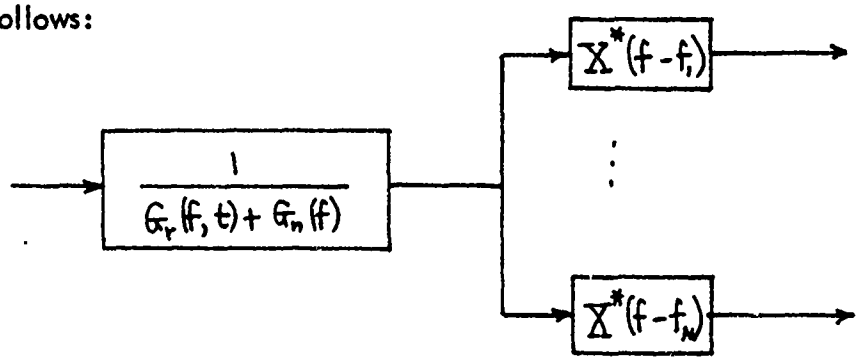

Figure 3. Optimum Receiver

The initial filter* in this processor varies slowly with time; this filter is followed by a bank of narrowband filters, each matched to a different frequency-shifted version of the transmitted signal. The separation between frequency shifts, $f_{k+1} - f_k$, must be less than the inverse signal duration, and the total number of frequency shifts must cover the expected range of Doppler shifts of the target.

The maximum SIR is obtained by substituting (21) in (20):

$$SIR_1 = 2R^2 \int df \, \frac{|X(f-f_d)|^2}{G_r(f,t) + G_n(f)} . \tag{22}$$

Recall that reverberation spectrum $G_r(f,t)$ is given by (16) in terms of the transmitted signal energy density spectrum.

Maximization of SIR_1 by choice of transmitted signal energy density spectrum $|X(f)|^2$, subject to fixed transmitted energy E_x, is not possible in general. One special case which can be solved, however, is when doppler shift $f_d = 0$ and when the reverberation channel does not spread in frequency. Then

$$\sigma_r(f,t) = \delta(f)\,\sigma_1(t), \tag{23}$$

and from (16),

$$G_r(f,t) = \tfrac{1}{4}\sigma_1(t)\,|X(f)|^2 . \tag{24}$$

---

*This is not a whitening filter; the whitening filter has transfer function $[G_r(f,t)+G_n(f)]^{-1/2}$.

In this special case (putting frequency band limit W in explicitly),

$$SIR_2 = 2R^2 \int_W df \frac{|X(f)|^2}{\frac{1}{4}\sigma_1(t)|X(f)|^2 + G_n(f)} . \tag{25}$$

This can be maximized for any noise spectrum; however, the general solution is not very informative, so we limit ourselves to white noise, over the signal band W. Then the optimum signal energy density spectrum is flat:

$$|X(f)|^2_{opt} = \frac{2E_x}{W} , \tag{26}$$

regardless of reverberation function $\sigma_1(t)$. The reverberation power is, from (17) and (23),

$$P_r(t) = \frac{1}{4}\sigma_1(t) E_x . \tag{27}$$

And for (real) white noise of double-sided level N_d, we have

$$G_n(f) = +N_d . \tag{28}$$

Substituting (26) - (28) in (25), there follows

$$SIR_3 = 2WR^2 \frac{E_x}{\frac{1}{4}\sigma_1(t)E_x + 2WN_d} = 2WR^2 \frac{E_x}{P_r(t) + P_n} , \tag{29}$$

where P_n is the real noise power received in a band W.

For a reverberation-limited environment, $P_r(t) >> P_n$, and

$$SIR_3 \cong \frac{8R^2}{\sigma_1(t)} W. \tag{30}$$

Since R^2 and $\sigma_1(t)$ are medium-controlled, the only variable under our control is the signal bandwidth W, which should be made large, according to (30)*. On the other hand, for a noise-limited environment, $P_n >> P_r(t)$, and

$$SIR_3 \cong \frac{R^2 E_x}{N_d} = \frac{E_s}{N_d} , \tag{31}$$

---

*Limitations on bandwidth W are discussed by Manasse (Ref. 3, p. 13); namely, the inherent granularity of some types of reverberation and the fact that the target is not a point, but a distributed reflector, serve to limit W.

where E_s is the received signal energy; this is a familiar result.

Generally, (29) appears as shown in Figure 4. Notice

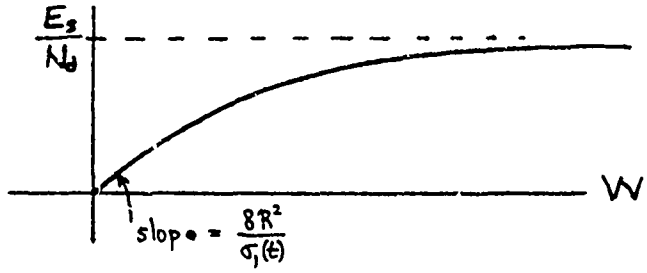

Figure 4. SIR_3 as a Function of Signal Bandwidth W

that signal duration or time distribution is not important, except that (26) must be satisfied in this case. This all applies for an energy-limited transmitter.

For a power-limited transmitter, $E_x = P_x T$, and (29) becomes

$$SIR_3 = \frac{R^2 P_x}{\frac{\sigma_1(t) P_x}{8W} + \frac{N_0}{T}} . \tag{32}$$

For a fixed signal time-bandwidth product $TW = K$, (32) is maximized by the choices

$$T = \sqrt{K \frac{8N_0}{\sigma_1(t) P_x}} \quad , \quad W = \sqrt{K \frac{\sigma_1(t) P_x}{8N_0}} , \tag{33}$$

yielding maximum value

$$SIR_4 = R^2 \sqrt{\frac{2K P_x}{\sigma_1(t) N_0}} . \tag{34}$$

This increases with the transmitter power only as $\sqrt{P_x}$, and with the time-bandwidth product only as $\sqrt{TW}$.

Although in this case we assumed no reverberation spreading, the same optimum signal (25) holds approximately for a unimodal spread of $\sigma(f,t)$ about $f = 0$. The reverberation power that is spread outside the band W can in fact be suppressed, and performance is slightly better than (29). However, as W is increased to improve reverberation suppression, (29) is again approached.

Another special case of (22) that can be solved for the optimum signal energy density spectrum, for all practical purposes, occurs as follows: suppose the

reverberation spreading in frequency is B_r Hz. Let the transmitted signal duration be T sec. Since the finest detail in signal energy density $|X(f)|^2$ is $1/T$ Hz, the finest detail in reverberation spectrum $G_r(f,t)$ in (16) is approximately $\frac{1}{T} + B_r$ Hz. Now if the doppler shift f_d is large enough that

$$\frac{1}{T} + B_r < f_d, \tag{35}$$

then there exists the possibility of packing $|X(f)|^2$ in a narrow frequency band (or bands) such that $|X(f-f_d)|^2$ does not overlap $G_r(f,t)$ for some values of doppler shift f_d. In this case, (22) becomes

$$SIR_4 \cong 2R^2 \int df \; \frac{|X(f-f_d)|^2}{G_n(f)} = \frac{R^2 E_x}{N_4} = \frac{E_s}{N_4}, \tag{36}$$

for white noise. Notice that the optimum signal energy density spectrum in this case is a narrowband spectrum, whereas the former case, (26) and (29), required a broadband signal.

The above two special cases suggest that a single "optimum" signal for the general case of unknown doppler ought to have both narrowband and broadband qualities. One such signal is a periodically-pulsed carrier. Then $|X(f)|^2$ extends over a broadband, but at the same time, has spectral regions of low level for good reverberation suppression. There is, however, the danger of ambiguous signal responses at periodically-spaced time delays and frequency shifts. (A narrowband CW pulse has extended range ambiguity, while linear FM has an elliptical ambiguity in range-velocity, and does not suppress reverberation very well, even for high Doppler targets).

The general SIR in a reverberation-limited environment is obtainable from (22) and (16) as

$$SIR_6 = 8R^2 \int df \; \frac{|X(f-f_d)|^2}{|X(f)|^2 \circledast \sigma_r(f,t)}.$$

In this case, the transmitted signal energy E_x cancels out. Thus individual pulse weighting, to improve reverberation suppression by spectrum shaping, does not detract from detectability in a reverberation-limited environment, even though the transmitted signal energy may be decreased.

4. RECEIVER OUTPUT REVERBERATION POWER FOR GENERAL SCATTERING FUNCTION

The reverberation waveform at the receiver input is given by (10). At the receiver filter output, the reverberation waveform is

$$z_r(t) = \frac{1}{2}\int dw\, h(t-w) r(w) = \frac{1}{4}\int dw\, h(t-w) \int d\tau\, h_r(\tau, w)\, x(w-\tau). \tag{37}$$

The output reverberation power is

$$P_{z_r}(t) = \frac{1}{2}\overline{|z_r(t)|^2} = \frac{1}{32}\iint dw_1\, dw_2\, h(t-w_1) h^*(t-w_2) \iint d\tau_1\, d\tau_2 \times$$

$$\overline{h_r(\tau_1, w_1)\, h_r^*(\tau_2, w_2)}\; x(w_1-\tau_1)\, x^*(w_2-\tau_2). \tag{38}$$

Employing (12) for the reverberation channel, and definition (6) for the signal-filter combination, this becomes

$$P_{z_r}(t) = \frac{1}{32}\iint d\tau\, d\nu\; \sigma_r(\nu, \tau) \left|\chi_{xh}(t-\tau, -\nu)\right|^2. \tag{39}$$

This relation allows for the interpretation in Figure 5.

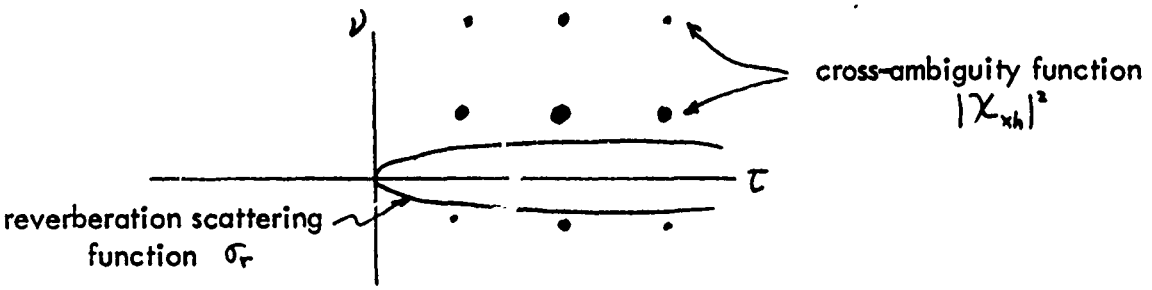

Figure 5. Scattering and Cross-Ambiguity Functions

If the reverberation scattering function and cross-ambiguity function do not overlap in τ, ν space for any time t, very little reverberation power results at the receiver filter output. This is the desired goal of signal-receiver design. Notice that since receiving filter H can be mismatched to the transmitted signal spectrum X, the cross-ambiguity function need not peak at the origin; thus the major ambiguous lobes indicated above can lie off the $\nu = 0$ axis.

In (39) above, no assumption about a slowly changing scattering function, $\sigma_r(\nu,\tau)$, with τ was necessary. However, in the case of a slowly changing σ_r,

the integral on τ in (39) becomes, upon use of (6),

$$\int d\tau\, \sigma_r(\nu,\tau) \iint dt_1\, dt_2\, x(t_1+t-\tau)\, x^*(t_2+t-\tau)\, h(-t_1)\, h^*(-t_2) \exp[i2\pi\nu(t_1-t_2)]$$

$$\equiv \iint dt_1 dt_2\, h(-t_1) h^*(-t_2)\, e^{i2\pi\nu(t_1-t_2)}\, \sigma_r\left(\nu, t+\tfrac{t_1+t_2}{2}\right) \int d\tau\, x(t_1+t-\tau)\, x^*(t_2+t-\tau)$$

$$= \int df\, |X(f)|^2 \iint dt_1 dt_2\, h(-t_1) h^*(-t_2) \exp[i2\pi(f+\nu)(t_1-t_2)]\, \sigma_r\left(\nu, t+\tfrac{t_1+t_2}{2}\right). \tag{40}$$

Now if the duration of receiver filter impulse response $h(\tau)$ is confined fairly near $\tau = 0$ in comparison with the time delay for σ_r to change, this further simplifies to

$$\sigma_r(\nu,t) \int df\, |X(f)|^2\, |H(f+\nu)|^2 \approx \sigma_r(\nu,t) \int df\, |X(f-\nu)|^2\, |H(f)|^2. \tag{41}$$

Substituting (41) in (39), and employing (16),

$$P_{a_r}(t) = \tfrac{1}{32} \int d\nu\, \sigma_r(\nu,t) \int df\, |X(f-\nu)|^2\, |H(f)|^2$$

$$= \tfrac{1}{8} \int df\, |H(f)|^2 \left[\tfrac{1}{4} |X(f)|^2 \otimes \sigma_r(f,t)\right]$$

$$= \tfrac{1}{8} \int df\, |H(f)|^2\, G_r(f,t), \tag{42}$$

in agreement with the reverberation part of (19). This result, (42), is a special case of the more general result (39).

5. PULSED CARRIER SIGNAL

The transmitted signal waveform $x(t)$ to be considered from here on will consist of a sequence of short duration pulses, centered at some carrier frequency f_o Hz; see Figure 6. The individual pulses may be

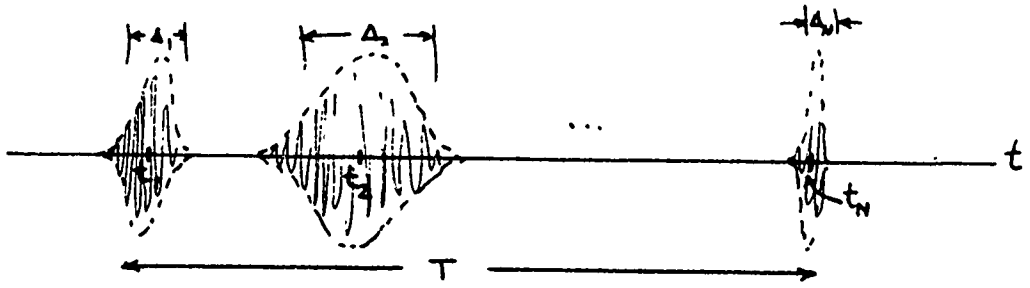

Figure 6. Transmitted Signal

frequency-shifted (as for Post Detection Pulse Compression). or they may all have a common carrier frequency (as for Amplitude Shift Keying).

6. RECEIVER PROCESSING FOR PULSED SIGNALS

6.1 Optimum Processing for Coherent Phases

If the phases of the individual signal pulses are maintained at definite relationships during transmission, and the medium does not perturb these relationships, the possibility of coherent receiver processing over the total signal duration T exists. The optimum receiver processor (for long observation times) then consists of a linear filter with transfer function given by (21), followed by an envelope detector and a continuous threshold comparison.

Several points about filter (21) should be noted. If the signal in Figure 6 is an equi-spaced pulse train on a common carrier, such as

$$x(t) = m(t)\left[\delta_{\frac{1}{f_r}}(t) \circledast p(t)\right] = m(t)\sum_{k=-\infty}^{\infty} p\left(t-\frac{k}{f_r}\right), \tag{43}$$

then

$$X(f) = M(f) \circledast \left[f_r\, \delta_{f_r}(f) P(f)\right] = f_r \sum_k P(kf_r)\, M(f-kf_r). \tag{44}$$

See Figures 7 and 8.

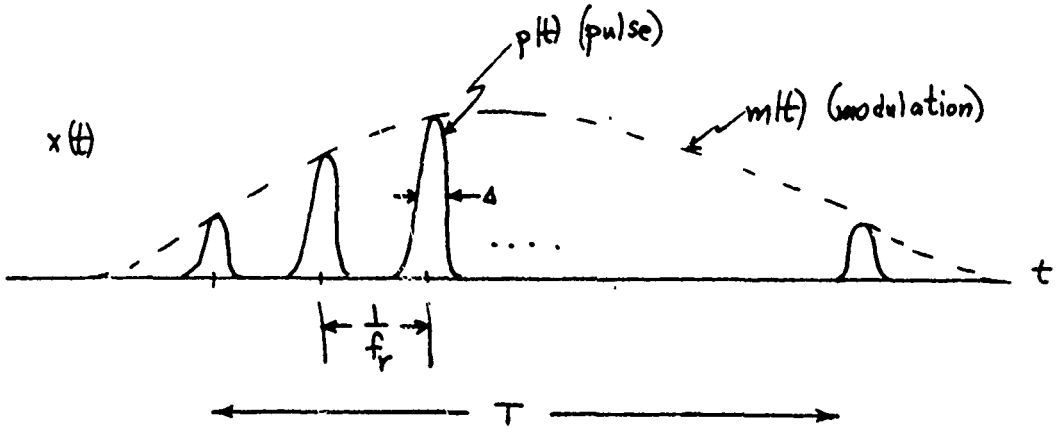

Figure 7. Equi-spaced Pulse Train Signal

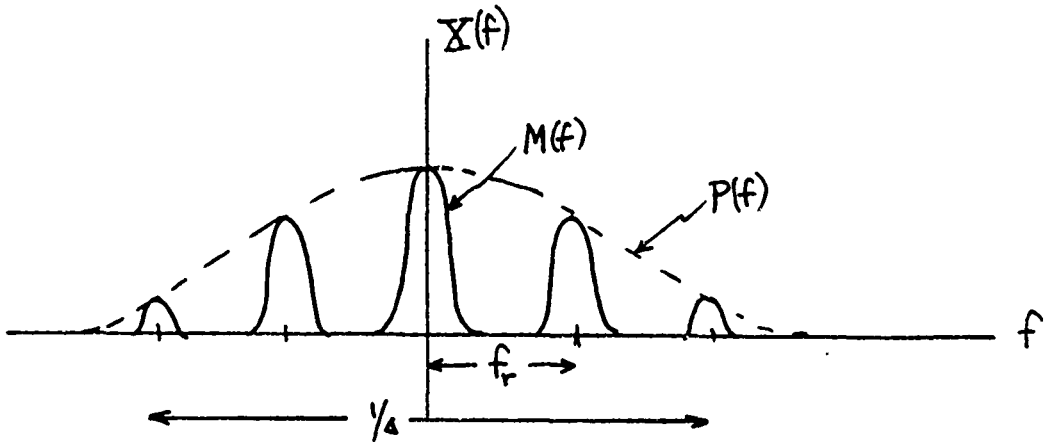

Figure 8. Voltage Density Spectrum of Signal

The impulse train

$$\mathcal{U}_{\Delta}(x) \equiv \sum_{K=-\infty}^{\infty} \delta(x-K\Delta). \tag{45}$$

From Figure 8 it is seen that $|X(f)|$ has several large spikes. Therefore the optimum filter (21) has large gains at certain frequencies (a "comb" filter depending on frequency shift f_d), and large notches at other frequencies. The notches are reverberation-rejection regions. (It should be noted that the impulse response duration of optimum filter (21) is T sec, the total transmitted signal duration.)

The importance of careful design of envelope modulation m(t) in Figure 7 is brought out by Figure 8. Namely, if m(t) is tapered in time such that $|M(f)|$ has low sidelobes, there exist frequency regions where $|X(f)|^2$ is extremely small. Target detection for these doppler shifts is thereby tremendously improved, because there is little reverberation power in the passband of the optimum filter. An example

of modulation design by Spafford (Ref. 4) shows over a 30 dB gain in comparison with rectangular modulation.

Also the importance of good pulse shaping p(t) is obvious by inspection of Figure 8. Namely, the distant sidelobes of $\mathcal{X}(f)$ depend on the function P(f). In order that a limited-bandwidth transmitter or receiver be capable of handling $\mathcal{X}(f)$ without significant effects on the spectrum, the distant sidelobes of $\mathcal{X}(f)$ should be small. Good choices of modulation m(t) and pulse p(t) are raised cosines (Hanning), for example.

If the reverberation power is so large that

$$G_r(f;t) \gg G_n(f) \quad \text{where } |\mathcal{X}(f-f_d)| \text{ is significant,} \tag{46}$$

in (21), then filter (21) can be designed without knowledge of the actual reverberation level; this is the reverberation-limited environment. On the other hand, if

$$G_r(f;t) \ll G_n(f) \quad \text{where } |\mathcal{X}(f-f_d)| \text{ is significant,} \tag{47}$$

the filter (21) is again independent of the reverberation level, and depends only on the noise spectrum; this is the noise-limited environment. In practice, where reverberation power P_r varies with time, the design of the optimum filter (21) is virtually impossible in the transition region between (46) and (47).

6.2 Sub-Optimum Processing for Coherent Phases

Let phase coherence between pulses be maintained at the transmitter*. However, suppose (a) this is unknown to the receiver or, (b) receiver complexity is desired reduced. Then a good sub-optimum processor consists of several filters, one matched to each of the individual pulses of the signal in Figure 6. The transfer function of the k-th filter (for long observation times) is given by

$$\frac{\mathcal{X}_k^*(f-f_d)}{G_r(f;t)+G_n(f)}, \tag{48}$$

where $\mathcal{X}_k(f)$ is the voltage density spectrum of the k-th pulse in Figure 6; see Ref. 5, App. C. The filters are followed by $\ln I_o$ envelope detectors, and delayed so as to line up the peak outputs simultaneously, and then compared with a threshold. (The difficulty of realizing $\ln I_o$ detectors usually is replaced by weighted sums of squares of envelopes.)

*Also let the medium not disturb the relative phase relationships of individual pulses.

Since the duration of the k-th pulse in Figure 6 is only Δ_k sec, the finest detail in the numerator in (48) is $1/\Delta_k$ Hz. This is much coarser than the numerator in the phase-coherent processor of (21). Thus each receiver filter for hypothesized incoherent phases possesses narrow deep notches for an equi-spaced pulse train, for reverberation rejection, but does not possess narrow regions of high gain. Rather, the numerator of (48) has the moderate slowly-changing gain prescribed by P(f) in Figure 8. However, it is important to note that since the finest detail in (48) is of frequency extent $1/T$ Hz (due to the denominator), the impulse response of each of the filters (48) is T sec, the total duration of the signal, even though it was originally designed for a single pulse. However, if the filter is realized as a cascaded system as in Figure 3, only the initial common filter need have this detail; the parallel filter bank has duration Δ_k seconds for the k-th filter. The performance curves for this sub-optimum processor are available*, and can be compared with the optimum processor of (21).

For the equi-spaced pulse train of Figure 7, the pulses are all identical, except for time delay and amplitude. Therefore, a single filter of the form (48) can be built, and its envelope output appropriately delayed and scaled before addition. This is still a relatively complicated filter, due to the narrow reverberation notches and the possible need for knowing the absolute reverberation level. (One could ignore the reverberation spectrum in the denominator in (48), and design the filters according to

$$\frac{X_k^*(f-f_d)}{G_n(f)} . \tag{49}$$

This processor is simpler, but will not perform very well in reverberation-limited environments.)

6.3 Optimum Processing for Incoherent Phases

If phase-coherence is not maintained at the transmitter, or if the medium causes significant phase perturbation over the signal duration T, then the reverberation spectrum is significantly different from $|X(f)|^2$. Specifically, for the pulse train of (43), (Figure 7), if the phase of each pulse is independently uniformly distributed over a 2π interval, the reverberation spectrum is

$$\tilde{G}_r(f) = P_r \frac{|M(f)|^2 \circledast |P(f)|^2}{\int du\,|P(u)|^2 \int dv\,|M(v)|^2} , \tag{50}$$

*Ref. 5; replace $G_n(f)$ everywhere by $G_n(f) + G_r(f,t)$.

where P_r is the reverberation power (and may vary slowly with time). A glance at Figure 8 shows this is a broad slowly-changing spectrum of width $\sim \frac{1}{\Delta} + \frac{1}{\Delta}$ Hz.

The optimum processor again consists of filters matched to the individual pulses, but now with transfer functions

$$\frac{X_x^*(f-f_d)}{G_n(f) + \tilde{G}_r(f)} . \qquad (51)$$

This is a broad filter of frequency extent $\frac{1}{\Delta}$ Hz, with no narrow characteristics whatsoever. Its impulse response duration is approximately Δ sec, that of an individual pulse. In order to get significant reverberation rejection, doppler shift f_d will have to be larger than $\frac{1}{\Delta}$ Hz, since this is the extent of the reverberation spectrum.

The filters outputs are square-law envelope detected, delayed, and summed, as before. Again, for the signal of Figure 7, a single filter will do, instead of the set (51), provided appropriate delays and weights are applied to the filter output.

7. A GENERIC RECEIVER PROCESSOR

For the equi-spaced pulse train of (43), the optimum processors for cases 6.2 and 6.3 above can be subsumed under that in Figure 9. The averager is characterized by impulse response $w(\tau)$, which could be a set of equi-spaced

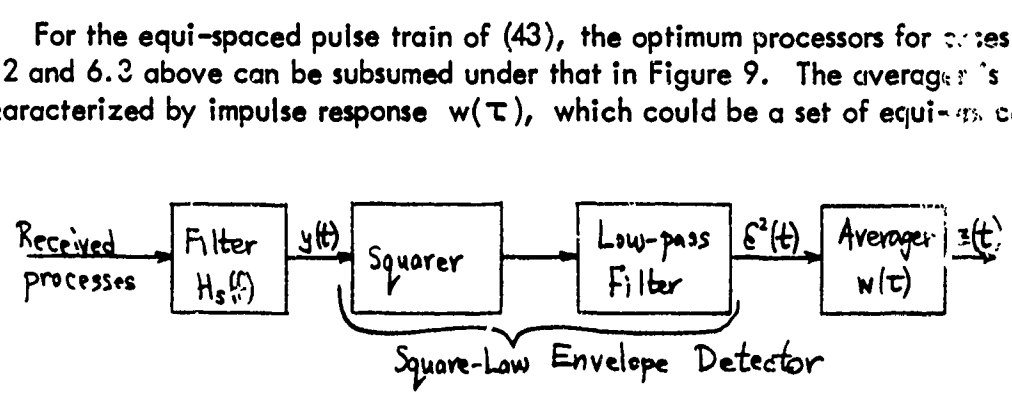

Figure 9. A General Processor

unequally-weighted impulses if desired, to realize the processors described earlier. Or the averager could be a box-car filter, when virtually no knowledge is available about the time-structure of the received signal. Similarly, filter $H_s(f)$ can be fairly broad-band, covering the expected frequency extent of the received signal; the subscript "s" denotes a particular frequency-shifted version,

$H_s(f) = H(f-f_s)$, to search for doppler. The range search is conducted by comparing $z_s(t)$ continuously with a threshold.

We investigate $z(t)$ at a general time instant t for a general filter $H(f)$ and averager $w(t)$. Thus time mismatch and frequency mismatch can be investigated. Time delay t_d and doppler shift f_d are general also.

A possible picture of $z(t)$ is given in Figure 10. The received signal

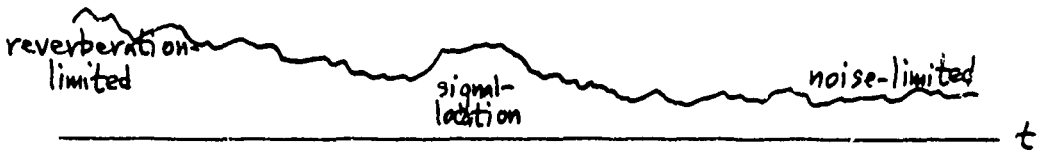

Figure 10. Processor Output

$s(t)$ is of the form (8) for a single path. $x(t)$ itself is composed of several sub-pulses, as in Figure 7.

The desired component of processor output $z(t)$ in Figures 9 and 10 is that due to the received signal $s(t)$. The reverberation and noise in the input raise the background level in $z(t)$, and add fluctuation; however they are not useful for signal detection. The desired output is therefore*

$$z_d(t) = w(t) \circledast \underline{e}_d^2(t) = w(t) \circledast |\underline{y}_d(t)|^2. \tag{52}$$

$$\underline{y}_d(t) = \tfrac{1}{2}\underline{h}_s(t) \circledast \left[\tfrac{V}{2} x(t-t_d) \exp(i 2\pi f_d t)\right]$$

$$= \tfrac{1}{2}\left[\underline{h}(t) \exp(i 2\pi f_s t)\right] \circledast \left[\tfrac{V}{2} x(t-t_d) \exp(i 2\pi f_d t)\right], \tag{53}$$

or using (6) for complex envelopes,

$$|\underline{y}_d(t)| = \tfrac{1}{2}\left|\chi_{xh}(t-t_d, f_s-f_d)\right| \frac{|V|}{2}. \tag{54}$$

---

*The underline denotes complex envelope in this section.

Then

$$z_d(t) = \frac{1}{4} w(t) \circledast \left| \chi_{xh}(t-t_d, f_s - f_d) \right|^2 \frac{|V|^2}{4}. \qquad (55)$$

Notice that the ambiguity function of $x(t)$ itself is not important. Rather, for this sub-optimum processor, the cross-ambiguity function between $x(t)$ and $h(-t)$ is the important quantity. The peak value of $z_d(t)$ is what detection capability depends upon.

For incoherent phases, the filter choice $H_s(f)$ can be guided by the result of (51). $H_s(f)$ can be approximately matched to a single pulse, frequency shifted by f_s Hz. The impulse response duration of $H_s(f)$ would then be approximately Δ seconds. The function $|\chi_{xh}(\tau, \nu)|^2$ is then indicated in Figure 11. (The decay with increasing $|\tau|$ is due to the decay of modulation

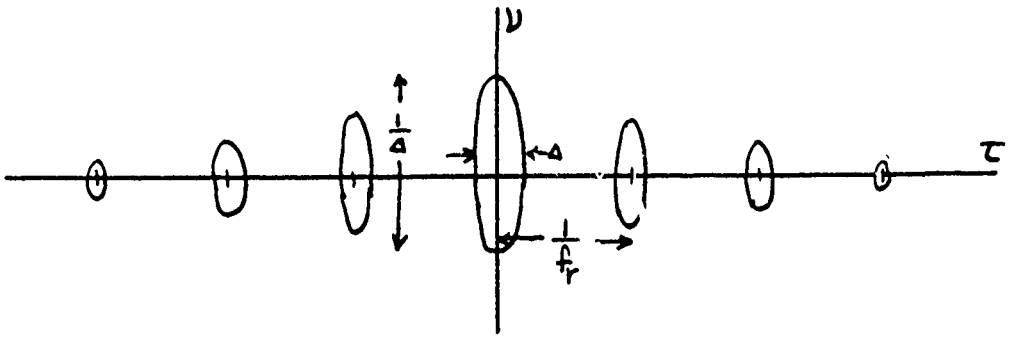

Figure 11. $|\chi_{xh}(\tau, \nu)|^2$ for Phase-Incoherent Pulses and Filter (51)

$m(t)$ in Figure 7.) Figure 11 indicates a very coarse function in ν, of width $1/\Delta$ Hz; thus target doppler is not possible to ascertain within $1/\Delta$ Hz in this case.

If the received phases are indeed coherent, but the filter $H_s(f)$ is not designed to account for this feature, either due to ignorance or complexity, Figure 11 still applies. Of course, the filter is not as good a reverberation-rejection filter as it could be.

For coherent phases, the filter choice $H_s(f)$ could be guided by (48). This filter has deep notches of width $1/T$ Hz, and therefore has an impulse response extending over T sec. The periodic frequency characteristic of $H_s(f)$, coupled with the periodic character of $X(f)$, leads to a cross-ambiguity function of the form in Figure 12. This is very similar to, but not identical with, the

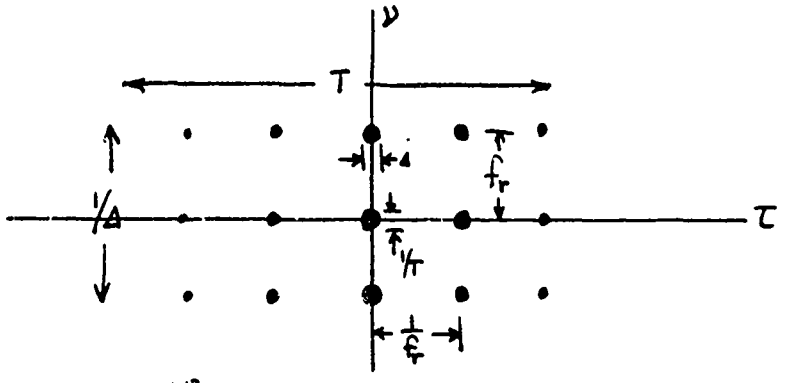

Figure 12. $|\chi_{xh}(\tau,\nu)|^2$ for Phase-Coherent Pulses and Filter (48)

ambiguity function of signal $x(t)$.

From (55), the desired output component is proportional to the convolution of $|\chi_{xh}|^2$ with $w(t)$. Thus $w(t)$ should have a series of sharp spikes separated by $1/f_r$ sec. in order to give rise to a large signal output at some (several) time instant; this is in keeping with the results mentioned above for the optimum processors.

The undesired component of output $z(t)$ in Figure 9 is the noise plus reverberation:

$$z_u(t) = w(t) \circledast e_u^2(t) = w(t) \circledast |y_u(t)|^2,$$

$$y_u(t) = \tfrac{1}{2} h_s(t) \circledast [\underline{n}(t) + \underline{r}(t)], \tag{56}$$

where $n(t)$ and $r(t)$ are the complex envelopes of the received noise and reverberation processes respectively. The mean value of $z_u(t)$ does not aid or hinder detection; it raises the average level in which a signal must be detected. However, the variance of $z_u(t)$ is a definite detriment to signal detection.

From (56), the spectrum of $z_u(t)$ is

$$|W(f)|^2 \times [\text{Spectrum of } |y_u(t)|^2]. \tag{57}$$

The correlation of $|y_u(t)|^2$ is, for Gaussian processes,

$$R^2_{y_u}(0) + |R_{y_u}(\tau)|^2, \tag{58}$$

giving spectrum

$$R^2_{y_u}(0)\,\delta(f) + \int dv\; G_{y_u}(v)\, G_{y_u}(v+f) \tag{59}$$

Therefore

$$\mathrm{Var}\{z_u(t)\} = \int df\, |W(f)|^2 \int dv\; G_{y_u}(v)\, G_{y_u}(v+f). \tag{60}$$

Now from (56),

$$\begin{aligned} G_{y_u}(f) &= \tfrac{1}{4}|H_s(f)|^2 \left[G_n(f) + G_r(f)\right] \\ &= \tfrac{1}{4}|H(f-f_s)|^2 \left[G_n(f) + G_r(f)\right], \end{aligned} \tag{61}$$

where $G_r(f)$ is the spectrum of the complex envelope of the reverberation, and is given by (6) for phase-coherent pulses, or by (50) for phase-incoherent pulses.

An alternative expression for (60) is afforded by

$$\mathrm{Var}\{z_u(t)\} = \int dt\, \phi_w(t) |R_{y_u}(t)|^2, \tag{62}$$

where

$$\phi_w(t) \equiv \int dx\; w(x)\, w(x-t). \tag{63}$$

Here $R_{y_u}(\tau)$ is the Fourier transform of (61).

A measure of the performance of the system of Figure 9 is then afforded by

$$SNR \equiv \frac{\left[\max_{t,f_s}\{z_d(t)\}\right]^2}{Var\{z_u(t)\}}, \tag{64}$$

The numerator and denominator of (64) are given by (55) and (60) or (62). Particular filters and averagers require numerical evaluation.

8. EXAMPLE OF A SUB-OPTIMUM PROCESSOR

Suppose $w(t) = 1$ for time interval T_a significantly greater than the signal duration. Also suppose $H(f) = 1$ for frequency interval W_f significantly greater than the bandwidth of the signal. Then

$$\underline{H}(f) = 2, \quad \chi_{xh}(\tau,\nu) \approx 2\chi(\tau), \tag{65}$$

giving

$$\max_{t,f_s}\{z_d(t)\} \approx \frac{1}{4}\int dt\,|\chi_{xh}(t-t_a,0)|^2\frac{|V|^2}{4} = \frac{1}{4}\int dt\,|V\chi(t-t_a)|^2 = 2E_s, \tag{66}$$

using (9). Also

$$\begin{aligned} Var\{z_u(t)\} &= \int dt\,\phi_w(t)|R_{y_u}(t)|^2 \approx \phi_w(0)\int dt\,|R_{y_u}(t)|^2 \\ &= T_a\int df\,|G_{y_u}(f)|^2 = T_a\int_{W_f} df\,[G_n(f)+G_r(f)]^2 \\ &\approx T_a\int df\,G_r^2(f) \quad \text{for a reverberation-limited environment.} \end{aligned} \tag{67}$$

Now since

$$\int df\,G_r(f) = 2P_r, \tag{68}$$

$$\mathrm{Var}\{z_u(t)\} \approx T_a\, 4P_r^2 \frac{\int df\, G_I^2(f)}{\left[\int df\, G_I(f)\right]^2} = 4P_r^2 \frac{T_a}{W_r}, \tag{69}$$

where W_r is the effective bandwidth of the reverberation. Then

$$SNR \approx \frac{E_s^2}{P_r^2} \frac{W_r}{T_a}. \tag{70}$$

There is no control over E_s/P_r, which is independent of the transmitted power However, W_r can be increased by widening the signal bandwidth, since the reverberation spectrum is related to the signal spectrum. T_a can be decreased only to the point where T_a is the signal duration. SNR also depends weakly on filter bandwidth W_f, since the noise power out of the filter increases with W_f.

9. COMMENTS

Phase-coherent Amplitude Shift Keying has good potential in reverberation because the reverberation spectrum is collected in a few narrow bands where it can be rejected. This is not possible with linear FM or CW. In order that the reverberation be peaked in frequency, it is necessary that phase coherence be maintained in the received process over the total signal duration T. That is, we must have, for the reverberation process,

$$B_r < \frac{1}{T}, \tag{71}$$

where B_r is the frequency smear of the reverberation channel. This causes only slight spreading of the reverberation spectrum corresponding to Figure 8. If $B_r > 1/T$, the reverberation spectrum smears, and rejection is degraded. If B_r is so large that $B_r > f_r$, then $\frac{1}{B_r} < \frac{1}{f_r}$, and random phase perturbations of each pulse in Figure 7 occurs; the corresponding reverberation spectrum is then given by (50). Now reverberation rejection is impossible.

The signal channel smear corrupts the received target echo if it is large. The optimum processing must be on a pulse-by-pulse basis, as considered earlier.

If the target echo is made up of multipath arrivals, there will be two (or more) signal response terms in desired output $z_1(t)$. The averager $w(t)$ can incoherently combine these outputs for improved signal detection capability.

10. REFERENCES

1. A. H. Nuttall and D. W. Hyde, "Operating Characteristics for Continuous Square-Law Detection in Gaussian Noise," NUSC Tech. Report 4233, 3 Apr 1972.

2. A. W. Ellinthorpe and A. H. Nuttall, "Theoretical and Empirical Results on the Characterization of Undersea Acoustic Channels," First IEEE Annual Comm. Conv., Boulder, Color., pp. 585-591, Jun 1965.

3. R. Manasse, "The Use of Pulse Coding to Discriminate Against Clutter," MIT Lincoln Lab. Group Report No. 312-12 (Rev. 1), 7 June 1961.

4. L. J. Spafford, "Optimum Radar Signal Processing in Clutter," IEEE Trans. on Info. Th., Vol. IT-14, No. 5, pp. 734-743, September 1968.

5. A. H. Nuttall, "ROC for Phase-Incoherent Detection of Multiple Observations," NUSC Tech. Memo. No. TC-179-71, 28 September 1971.

6. E. C. Westerfield, R. H. Prager, and J. L. Stewart, "Processing Gains Against Reverberation (Clutter) Using Matched Filters," IEEE Trans. on Info. Th., Vol. IT-6, No. 3, pp. 342-348, June 1960.

7. A. W. Rihaczek, "Radar Resolution Properties of Pulse Trains," Proc. IEEE, Vol. 52, No. 2 , pp. 153-164, February 1964.

8. H. L. Van Trees, "Optimum Signal Design and Processing for Reverberation-Limited Environments," IEEE Trans. Military Electronics, Vol. MIL-9, pp. 212-229, July/October 1965.

9. W. D. Rummler, "Clutter Suppression by Complex Weighting of Coherent Pulse Trains," IEEE Trans. on Aero. and Elec. Sys., Vol. AES-2, No. 6, pp. 689-699, November 1966.

10. M. Ares, "Optimum Burst Waveforms for Detection of Targets in Uniform Range-Extended Clutter, IEEE Trans. on Aero. and Elec. Sys., Vol. AES-3, No. 1, pp. 138-141, January 1967.

11. D. Middleton, "A Statistical Theory of Reverberation and Similar First-Order Scattered Fields, Parts I and II," IEEE Trans. on Info. Th., Vol. IT-13, No. 3, pp. 372-414, July 1967.

12. D. F. Delong and E. M. Hofstetter, "On the Design of Optimum Radar Waveforms for Clutter Rejection," IEEE Trans. on Info. Th., Vol. IT-13, No. 3, pp. 454-463, July 1967.

13. W. D. Rummler, "A Technique for Improving the Clutter Performance of Coherent Pulse Train Signals," IEEE Trans. on Aero. and Elec. Sys., Vol. AES-3, No. 6, pp. 898-906, November 1967.

14. C. W. Helstrom, Statistical Theory of Signal Detection, Pergamon Press, N.Y., Second Edition, 1968.

15. H. Urkowitz, "Some Properties and Effects of Reverberation in Acoustic Surveillance," IEEE Trans. on Aerospace and Electronic Systems, Vol. AES-4, No. 1, pp. 112-122, January 1968.

16. C. A. Stutt and L. J. Spafford, "A 'Best' Mismatched Filter Response for Radar Clutter Discrimination," IEEE Trans. on Info Th., Vol. IT-14, No. 2, pp. 280-287, March 1968.

17. L. E. Brennan and I. S. Reed, "Optimum Processing of Unequally Spaced Radar Pulse Trains for Clutter Rejection," IEEE Trans. on Aero. and Elec. Sys., Vol. AES-3, No. 3, pp. 474-477, May 1968.

18. H. Urkowitz, "Some High-Velocity Clutter Effects in Matched and Mismatched Receivers," IEEE Trans. on Aero. and Elec. Sys., Vol. AES-4, No. 3, pp. 481-485, May 1968.

19. R. L. Mitchell and A. W. Rihaczek, "Clutter Suppression Properties of Weighted Pulse Trains," IEEE Trans. on Aero. and Elec. Sys., Vol. AES-4, No. 6, pp. 822-828, November 1968.

20. D. F. Delong and E. M. Hofstetter, "The Design of Clutter-Resistant Radar Waveforms with Limited Dynamic Range," IEEE Trans. on Info. Th., Vol. IT-15, No. 3, pp. 376-385, May 1969.

21. D. F. Delong, "Design of Radar Signals and Receivers Subject to Implementation Errors," IEEE Trans. on Info. Th., Vol. IT-16, No. 6, pp. 707-711, November 1970.

22. R. A. Altes, "Suppression of Radar Clutter and Multipath Effects for Wide-Band Signals," IEEE Trans. on Info. Th., Vol. IT-17, No. 3, pp. 344-345, May 1971

23. R. J. McAulay and J. R. Johnson, "Optimal Mismatched Filter Design for Radar Ranging, Detection, and Resolution," IEEE Trans. on Info. Th., Vol. IT-17, No. 6, pp. 696-701, November 1971.